Valence-bond Isomer Chemistry. Part 10.[1] Kinetics and Thermodynamics of the Thermal Gas-phase Interconversion of Hexakis(pentafluoroethyl)benzene and its *para*-Bonded (' Dewar ') Isomer [2]

By **Abdul-Majeed M. Dabbagh, William T. Flowers, Robert N. Haszeldine,* and Peter J. Robinson,** Department of Chemistry, The University of Manchester Institute of Science and Technology, Manchester M60 1QD

The gas-phase interconversion of hexakis(pentafluoroethyl)benzene (1) and its *para*-bonded isomer (2) is a clean reversible isomerisation at 7—60 mmHg and 457—602 K. Measurements of the equilibrium constant give $\Delta H^{\ominus}$ = 37.6 ± 0.3 kJ mol^{-1} and $\Delta S^{\ominus}$ = 68.2 ± 0.5 J K^{-1} mol^{-1} for reaction (1), error limits being standard errors. The reaction at 457—525 K shows reversible first-order kinetics with the Arrhenius equations (i) and (ii) for the forward and backward reactions, respectively. The reaction is completely unaffected by packing the vessel with

$$\log_{10}k_1/s^{-1} = (16.25 \pm 0.12) - (186.6 \pm 1.1)\ \text{kJ mol}^{-1}/RT \ln 10 \quad \text{(i)}$$

$$\log_{10}k_{-1}/s^{-1} = (12.99 \pm 0.16) - (151.7 \pm 1.5)\ \text{kJ mol}^{-1}/RT \ln 10 \quad \text{(ii)}$$

glass tubes or by adding but-2-ene to the system, and it is concluded that the interconversions are unimolecular. The reaction probably involves a biradical intermediate, and the rate-determining activated complex is similar in its structure to the *para*-bonded isomer rather than the benzene.

THE thermal reactions of the valence-bond isomers of benzene derivatives have been the subject of various kinetic and thermochemical investigations in recent years, but the scope of such studies has always been limited by the high thermodynamic instability of the non-aromatic isomers, as a result of which the thermal interconversions can be studied only in the aromatisation direction. Kinetic studies on the *para*-bonded → aromatic conversion give activation parameters, but not thermodynamic parameters for the overall reaction. Thermal analysis techniques can yield both the aromatisation activation parameters and the overall enthalpy of reaction, but even at best leave the overall entropy change undetermined. In the present paper we report comprehensive kinetic and equilibrium studies on the interconversion of hexakis(pentafluoroethyl)benzene (1) and its *para*-bonded (' Dewar ') isomer hexakis(pentafluoroethyl)bicyclo[2.2.0]hexa-2,5-diene (2). These compounds provide an unusual system in which the *para*-bonded isomer can be formed by purely thermal reaction of the benzene,[3] making possible the first equilibrium studies on a reaction of this type, along with detailed kinetic measurements on the reaction in both directions.

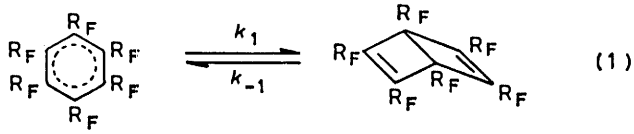

(1) benzene (2) *para*-bonded isomer

$R_F = C_2F_5$

EXPERIMENTAL

The apparatus used for kinetic and equilibrium experiments was similar to those described previously,[4] but was specially constructed for study of the high boiling reactant and product, which had useful vapour pressures only at temperatures above 440 K (Table 1). It consisted essentially of a spherical Pyrex reaction vessel (7.2 cm i.d.) enclosed in a circulating-air furnace [5] (maintained constant to ±0.1 K during a run by a Sirect Mark I proportional controller), and connected to a gas handling system enclosed in an air thermostat controlled at *ca.* 440 K by a Sunvic RT2 controller. The pressures in the line and in the reaction vessel were recorded by transducer gauges (S.E. laboratories SE 180/5 psi), which were themselves enclosed in the thermostat and had sensitivities of 26.3 and 16.1 mmHg † for recorder full scale deflections on the ranges normally used. The thermostat also contained storage bulbs and a gas-sampling valve (g.s.v.) (Dohrmann–Loenco L-208-8) for direct injection of reaction mixtures to the g.l.c. The taps in this section were Springham's greaseless stopcocks with Viton-A diaphragms, operated from outside the thermostat by extension handles.

Analysis.—Analysis was by g.l.c. on a Pye–Unicam model 104 with dual heated flame-ionisation detectors [these were much more sensitive to (1) and (2) than katharometric detectors]. Mixtures for analysis were expanded directly from the reaction vessel into the sampling loop of the gas chromatograph *via* the g.s.v. to minimise losses of materials and alteration of the product ratios (as might happen, *e.g.*, if the mixtures were condensed then evaporated and remixed). The output from the chromatograph was integrated by a Kent Chromalog Mark I integrator.

In the early stages of the work, major problems were encountered with condensation in the thermostat and the g.l.c., particularly with (1) (on account of its low vapour pressure: Table 1). Distorted peaks (*e.g.* flat-topped) and irreproducible calibrations were obtained. In order to eliminate these problems, the detector head was modified to minimise the distance between the g.s.v. and the column, and great care was taken to ensure uniform heating in the thermostat, the pipe connecting the g.s.v. with the injection port, and the injection port itself. Excessive heating at any point had to be avoided since reaction (1) proceeds at a measurable rate at temperatures not much above 440 K. Sample pressures were limited to a maximum of 3 mmHg

† 1 mmHg = 133.32 Pa.

TABLE 1

Vapour pressure and derived data for (1) and (2)

Isomer	Temp. range	A [a]	B/K [a]	L/kJ mol^{-1} [b]	B.p./K [c]	Tr/ J K^{-1} mol^{-1} [d]
(1)	416—471 (solid)	17.894	7 224.1	138.3	(481) [c]	
	471—492 (liquid)	8.997	3 032.3	58.1	495.8	117
(2)	329—397 (solid)	9.045	2 937.4	56.2	(477) [c]	
	397—466 (liquid)	8.369	2 666.2	51.0	485.8	105

[a] Constants in the equation $\log_{10}$ (vapour pressure/mmHg) $= A - B/T$. [b] Latent heat of sublimation or evaporation. [c] Or normal sublimation temperature (extrapolated) for solid phase. [d] Trouton constant.

in a sample loop of only 0.15 cm^3 volume. With these precautions, successful injections of the compounds were made on many different columns, *e.g.* PEGA, Apiezon L, and DC-QF1. The column used for quantitative analysis was 10.2 m × 6 mm i.d. of 10 wt.% silicone oil SE30 on Celite (80—100 mesh), operated at 418 K with a carrier gas flow of 60 cm^3 min^{-1} at s.t.p. [retention times: (2), 8.2 min, (1), 10.4 min]. Repeated treatment of columns with dichlorodimethylsilane was necessary for reproducible results.

Calibrations for both (1) and (2) were slightly non-linear, but reproducible peaks were obtained for injection pressures in the range 0.2—3.0 mmHg, corresponding to the least-mean-square quadratic calibration equations (2) and (3)

$$P_B/\text{mmHg} = 0.101\,4 + 6.226\,A_B + 1.430\,A_B^2 \quad (2)$$

$$P_D/\text{mmHg} = 0.123\,0 + 5.492\,A_D + 1.531\,A_D^2 \quad (3)$$

where P_B and P_D = injection pressure of the benzene or the *para*-bonded isomer and A_B and $A_D = 10^{-3} \times$ integrator count for the corresponding peaks.

Materials.—Compounds (1),[6] purified by vacuum sublimation, and (2), prepared by passing (1) in the vapour phase at low pressure over silica chips at 670 K and purified by recrystallisation from carbon tetrachoride, were pure by g.l.c. on several columns, i.r. spectroscopy,[3,6] and tensimetric examination. In the last, vapour pressures were recorded both for the liquid and solid phases of each isomer, as shown in Table 1. From the intersection of the linear plots the m.p. were determined as 471 and 397 K for (1) and (2) respectively (lit., 471—472,[6] 395—397 K [3]), and from the latent heats of evaporation and sublimation, the latent heats of fusion are 80.2 and 5.2 kJ mol^{-1} respectively.

RESULTS

Preliminary experiments showed that reasonable rates of interconversion were obtained at temperatures above *ca.* 450 K. No pressure change was observed during any runs at temperatures between 450 and 602 K, no carbonaceous deposit was formed, and no compounds other than (1) and (2) were ever detected in the products of these runs. It is clear from these observations that the interconversion proceeds cleanly according to the simple stoicheiometry of reaction (1).

Reactions at 621 K for several hours or 668 K for 20 min resulted in extensive breakdown to give, *inter alia*, perfluorobutane and perfluoro-1,4,5,6-tetraethyl-2,3-diethylidenebicyclo[2.2.0]hex-5-ene.[7] The reaction at these temperatures was sensitive to surface effects and probably proceeds by a free-radical mechanism, but no detailed studies were made.

Equilibrium Studies.—The equilibrium between (1) and (2) was measured at total pressures of 10—40 mmHg in the temperature range 457—602 K, over which range the *para*-bonded isomer comprised between 16 and 67% of the total material present at equilibrium (Table 2). Equilibrium was attained in <1 s at the higher temperatures, but required

TABLE 2

Equilibrium constants ($K_{eq} = p_2/p_1$)

Temp./K	No. of measurements	% *para*-Bonded isomer at equilibrium	$\bar{K}_{eq}$	$\sigma(\bar{K}_{eq})$ [a]
456.7	4	16.0	0.191	0.002
467.2	3	19.2	0.237	0.002
476.9	6	21.4	0.272	0.002
477.6	8	22.0	0.283	0.001
489.5	4	25.3	0.339	0.001
506.2	4	31.5	0.460	0.003
510.4	5	33.2	0.497	0.001
514.7	3	34.7	0.532	0.001
525.7	4	39.3	0.646	0.001
536.2	3	44.1	0.789	0.003
546.2	3	48.4	0.936	0.001
562.2	2	54.3	1.190	0.003
575.2	3	58.7	1.420	0.001
590.0	5	63.3	1.725	0.004
602.2	3	66.9	2.017	0.04
621.4	5	68.0 [b]	2.126 [b]	0.01
667.2	3	76.8 [b]	3.302 [b]	0.03

[a] Standard error of the mean. [b] Inaccurate data; see text.

many hours at the lower temperatures. Typical plots showing the progress of the reaction towards equilibrium are shown in Figure 1, and demonstrate very clearly how initial

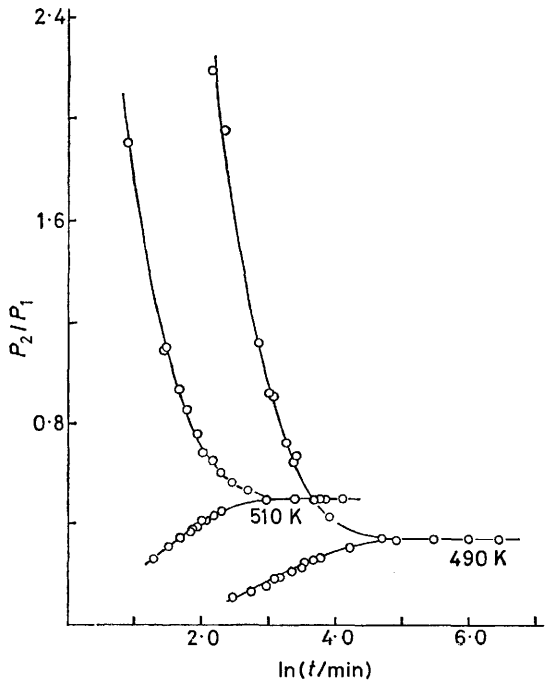

FIGURE 1 Approach to equilibrium from both sides

mixtures of any composition attained the same equilibrium composition at a given temperature. The final pressure ratio thus corresponds to the equilibrium constant K_{eq} defined by equation (4), in which p_1 and p_2 = partial

$$K_{eq} = p_2/p_1 \quad (4)$$

pressures of (1) and (2), respectively. An excellent straight line was obtained when ln K_{eq} was plotted against the reciprocal of the absolute temperature, corresponding to equation (5). The values obtained for the mean enthalpy change, $\Delta H^{\ominus}$, and entropy change $\Delta S^{\ominus}$, for the reaction in the temperature range 457—602 K are $\Delta H^{\ominus} = 37.6 \pm 0.3$ kJ

$$\ln K_{eq} = \Delta S^{\ominus}/R - \Delta H^{\ominus}/RT \quad (5)$$

mol^{-1}, $\Delta S^{\ominus} = 68.2 \pm 0.5$ J K^{-1} mol^{-1}; the $\pm$ represent standard errors as in Table 6. Deviations from the straight line were observed at temperatures above 602 K. The reaction is very fast at these temperatures ($t_{\frac{1}{2}}$ estimated to be *ca.* 0.4 s at 602 K), and there could well be an appreciable change of composition during the short time required for the mixture to pass from the reaction vessel through the capillary tube into the line for analysis. The points at the highest temperatures should therefore correspond to temperatures lower than those recorded, as is observed.

TABLE 3

Comparative data for kinetic plots at 477.6 K

		10^4 slope/s^{-1}		
Starting compound	ln F_0	Individual [a]	One way combined [b]	Both ways combined [c]
(1)	0.057	3.276	3.305	3.317
	0.057	3.276		
	0.083	3.303		
	0.228	3.200		
(2)	0.254	3.324	3.374	
	0.299	3.311		
	0.208	3.262		

[a] Individual plots [Figures 2(a) and (b)]. [b] Combined plot [equation (6)] for one direction only. [c] Combined plot [Figure 2(c)] for all runs at this temperature.

Kinetic Studies.—Kinetic runs were performed by analysing the products of many individual reactions carried out for different times at a given temperature, starting from both sides [(1) ⟶ (2) and (2) ⟶ (1)], at temperatures from 457 to 526 K and with total initial pressures from 7 to 62

$$\ln (F_0/F_t) = (k_1 + k_{-1})t \quad (6)$$

mmHg. The results were analysed as a reversible first-order reaction (1), for which the differential equation

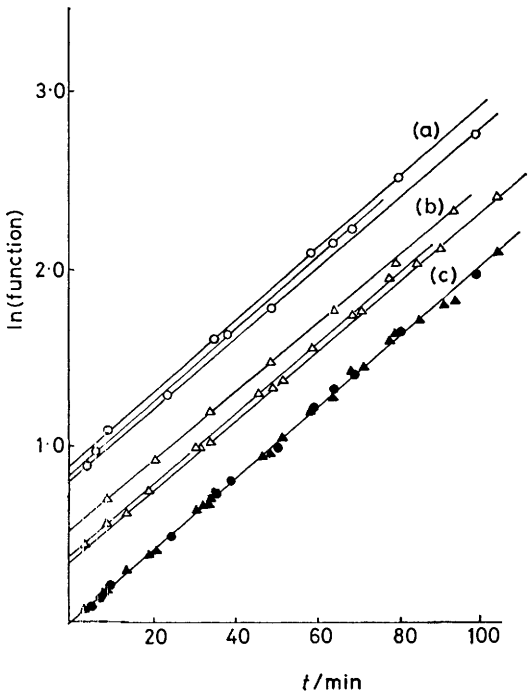

FIGURE 2 Kinetic plots at 477.6 K: (a) ln F_t *versus* t for runs starting with (1), shifted up by 0.6 log units (○); (b) ln F_t *versus* t for runs starting with (2), shifted up by 0.3 log units (△); (c) corresponding plots of ln(F_0/F_t) *versus* t (● and ▲)

$-dp_1/dt = k_1p_1 - k_{-1}p_2$ leads to the integrated equation (6) where $F_t = [(K_{eq} + 1)\theta_t - 1]/K_{eq}$, $\theta_t = p_1/(p_1 + p_2)$, and subscript 0 refers to $t = 0$. For runs starting with (1), $-\ln F_t$ was plotted against time; each plot was linear, and all the runs at a given temperature had the same slope ($k_1 + k_{-1}$) (*e.g.* Figure 2, upper curves). For runs starting with (2) the corresponding variation, with $K'_{eq} = 1/K_{eq}$ and $\theta'_t = 1 - \theta_t$, behaved in the same way (*e.g.* Figure 2, middle curves). The initial (1) and (2) in each run always contained small amounts of the other compound, formed by isomerisation during storage or transfer through the heated gas-handling line. The plots therefore have variable non-zero intercepts ln F_0(= 0 only if $\theta_0 = 1$). Using these intercepts, a common plot of ln(F_0/F_t) against time can now be constructed for all the runs at a given temperature, starting from either isomer (*e.g.* Figure 2, lower plot). Such plots showed very good agreement between runs and were linear for as long as followed (two or three half-lives), confirming the simple reversible first-order kinetic behaviour. Some comparative data illustrating the self-

TABLE 4

Overall rate constants ($k_1 + k_{-1}$)

		Initial	$10^4(k_1 + k_{-1})$/s^{-1}			
Temp./K	No. of runs	pressure/ mmHg	(1)→(2)	(2)→(1)	Combined	$10^4\sigma$/s^{-1} [a]
456.7	5	12.0—19.6		0.489	(0.489)	0.003
467.2	8	9.4—21.0	1.363	1.371	1.366	0.006
477.6	12	9.6—60.1	3.37	3.31	3.32	0.02
489.5	6	10.5—15.5	8.98	9.18	9.10	0.08
510.4	14	8.4—62.0	43.0	43.6	43.4	0.3
514.7	7	7.0—15.4	59.4	60.0	59.5	0.5
525.7	5	9.0—15.7	133		(133)	6.5 [b]

[a] Standard error of slope of combined plot; see also the text. [b] The reaction was very fast at this temperature and the plot shows substantially more scatter than those at other temperatures.

consistency are given in Table 3, and the overall rate constants for each temperature are given in Table 4.

At 477.6 and 510.6 K, runs were carried out over as wide a pressure range as possible (Table 4); the rate constants so obtained were independent of the total initial pressure, and this further confirms the first-order character of the reactions involved. The individual rate constants (k_1 and k_{-1}) were calculated from the combined overall rate constant ($k_1 + k_{-1}$) and the equilibrium constant K_{eq} at each temperature, and are summarised in Table 5. Arrhenius plots for k_1 and k_{-1} were excellent straight lines, corresponding to the parameters given in Table 6.

In Tables 4, 5, and 7 the standard error σ of the slope of a plot represents simply the uncertainty due to the scatter of the points about the regression line, and is thus a measure of the reproducibility of the result rather than its absolute accuracy. A further error is introduced by the uncertainty in the true value of K_{eq} (Table 2), which is used in the calculation of F_t and therefore ($k_1 + k_{-1}$), and also in calculating the individual rate constants from ($k_1 + k_{-1}$); this additional uncertainty is small, however.

Effect of Surfaces and Inhibitor.—The homogeneity of the reaction was investigated by runs carried out from both sides in a reaction vessel packed with glass tubes (surface : volume ratio 17.7 cm^{-1}, *cf.* 0.83 cm^{-1} for the unpacked vessel). To test for free-radical mechanisms, the reaction starting from the *para*-bonded side was studied in the presence of added *trans*-but-2-ene; the reactant and the additive were mixed in the reaction vessel itself.

TABLE 5

Individual rate constants

Temperature/K	10^4k_1/s^{-1}	$10^4\sigma_1$/s^{-1} [a]	10^4k_{-1}/s^{-1}	$10^4\sigma_{-1}$/s^{-1} [a]
456.7	0.0784	0.0005	0.411	0.002
467.2	0.260	0.001	1.095	0.005
477.6	0.731	0.004	2.59	0.01
489.5	2.30	0.02	6.80	0.06
510.4	14.4	0.09	29.0	0.2
514.7	20.7	0.2	38.8	0.3
525.7	52	3	81	4

[a] As in Table 4.

TABLE 6

Arrhenius parameters and entropies of activation [a,b]

Reaction	$\log_{10}(A/s^{-1})$	E_a/kJ mol^{-1}	$\Delta S^{\ddagger}$/J mol^{-1} K^{-1}
(1)→(2)	16.25 ± 0.12	186.6 ± 1.1	53.8 ± 2.4
(2)→(1)	12.99 ± 0.16	151.7 ± 1.5	−8.7 ± 3.0

[a] $\Delta S^{\ddagger}$ at 490 K,[8b] taking statistical factors to be unity (see Discussion). [b] The error limits quoted correspond to the standard errors of the slopes or intercepts of the appropriate plots, representing the results at each temperature by a single point with unit weighting.

TABLE 7

Effect of surface : volume ratio and inhibitor

Temp./K	Type of run	No. of runs	Total pressure/mmHg	$10^4(k_1 + k_{-1})$/s^{-1}	$10^4\sigma$/s^{-1} [a]
477.6	Standard	12	10—60	3.32	0.02
	Packed	4	13—29	3.47	0.02
	Butene	5	27—124 [b]	3.14	0.02
510.4	Standard	14	8—62	43.4	0.3
	Packed	6	11—15	41.2	0.3
	Butene	4	26—35 [c]	43.4	0.3

[a] As in Table 4. [b] Butene : reactant = 0.33—1.9. [c] Butene : reactant = 0.85—2.0.

The function plots for these runs were linear up to two or three half-lives, and the overall rate constants were within experimental error the same as those obtained in the unpacked vessel with inhibitor absent (Table 7). It is concluded that the interconversion processes are homogeneous and do not proceed to any measurable extent by free-radical mechanisms.

DISCUSSION

The interconversion of (1) and (2) is thus a clean reversible reaction at 457—602 K, and obeys reversible first-order kinetics with no evidence of free-radical or surface effects at 457—525 K. It is concluded that the forward and reverse reactions are unimolecular processes in their high pressure regions (as expected [8a] for molecules of this complexity, even at pressures much lower than those used here).

Overall Enthalpy and Entropy Changes.—The standard enthalpy and entropy changes for reaction (1) can be

TABLE 8

Overall enthalpy and entropy changes from kinetic and equilibrium studies

	Temp. range/K	$\Delta H^{\ominus}$/kJ mol^{-1}	$\Delta S^{\ominus}$/J K^{-1} mol^{-1}	Temp./K for $K_{eq} = 1$ or $k_1 = k_{-1}$
Kinetic studies	457—525	34.9 ± 1.9	62.6 ± 3.8	559
Equilibrium studies	457—525	35.8 ± 0.6	64.5 ± 1.2	555
	457—602	37.6 ± 0.3	68.2 ± 0.5	552

calculated from the activation parameters (Table 6) for the opposing reactions, and the values thus obtained are in very satisfactory agreement with those from the equilibrium studies (Table 8), especially if the latter are taken over the temperature range 457—525 K of the kinetic studies. It is interesting to note that thermal equilibrium favours the *para*-bonded isomer at temperatures above *ca.* 550 K, the kinetic and equilibrium data being in good agreement on this conclusion.

Although the present study provides the first complete energy and entropy profiles for this type of reaction, partial data have been obtained for other compounds, and in particular for the *para*-bonded to aromatic conversion of (3) to (4), studied by differential scanning calorimetry.[9-12]

(3) (4)

a; R = CH_3
b; R = F
c; R = CF_3

The enthalpy data for these systems are compared with those for reaction (1) in Figure 3. The higher ground-state energies of the *para*-bonded isomers in general, compared with the benzenes, are attributable to

the strained structure of the former, particularly at the central bond, where the orbital overlap is very small.[13] There are very large differences in $\Delta H^{\ominus}$ between the various systems in Figure 3, however, and it is noteworthy that the magnitude of $\Delta H^{\ominus}$ varies inversely with the size of the substituent groups, *i.e.* the smallest $\Delta H^{\ominus}$ corresponds to aromatisation of (2) with its large pentafluoroethyl substituents, while the largest $\Delta H^{\ominus}$ correspond to aromatisation of (3a) and (3b) with the relatively small methyl and fluorine substituents. Electronic effects would not be expected to produce such major variations in $\Delta H^{\ominus}$ [particularly in the series (3b), (3c), (1)] and the explanation is presumably in terms of steric effects.

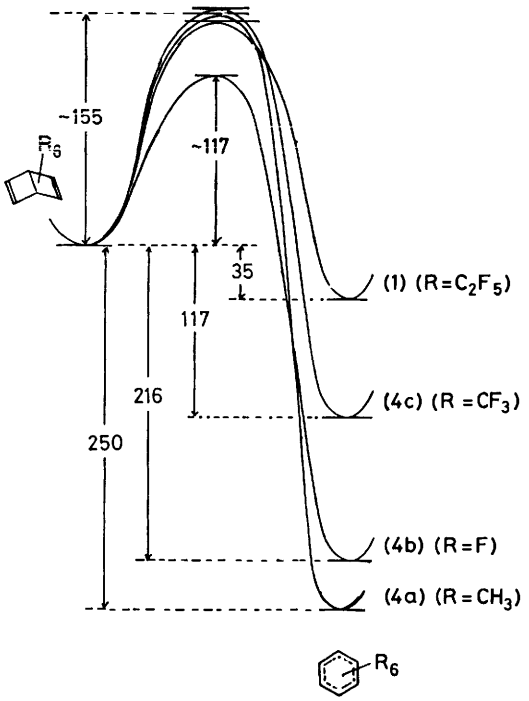

FIGURE 3 Energy profiles for the *para*-bonded ⇌ aromatic conversions (energies in kJ mol^{-1})

It can be postulated, however, that the substituent groups in all the non-aromatic isomers are sufficiently separated that steric repulsion among them is negligible. This suggestion is supported by the similar enthalpy changes observed for the prismane-to-*para*-bonded isomer conversion in the hexamethyl and hexakis(trifluoromethyl) series ($\Delta H^{\ominus} = -133$ and -130 kJ mol^{-1} respectively) [9,12] and by the similar activation energies for the *para*-bonded-to-benzene isomerisation of (2), (3a), and (3c). If this idea is correct, the differences in the observed $\Delta H^{\ominus}$ for the *para*-bonded-to-benzene conversion are mainly due to the relative steric crowding and non-bonded interaction of the bulky substituent groups present in the aromatic molecule itself. This interaction will raise the enthalpies of the benzenes relative to the corresponding *para*-bonded isomers, and produce the observed decrease in enthalpy difference with increasing size of the substituent. It is for these reasons that the energy levels of the *para*-bonded isomers have been equated in Figure 3, and the relatively crowded benzene molecules have been shown at different energy levels.

The thermal isomerisation of (1) to (2) seems at first sight surprising, and can only occur because the unfavourable $\Delta H^{\ominus}$ is small enough in this system to be overcome by the positive $\Delta S^{\ominus}$ at relatively low temperatures. The large positive entropy change for reaction (1) (+64 J K^{-1} mol^{-1}) can be explained in terms of steric crowding of the six pentafluoroethyl groups in the benzene molecule which must severely restrict the rotational freedom in the molecule. Indeed, a model of the benzene cannot be constructed with conventional bond angles and atomic radii, and this suggests appreciable distortion of the molecule, possibly even affecting the benzene ring as well as the substituents. In the *para*-bonded isomer, the steric crowding is reduced by folding of the ring system across the central bond, and this must lead to increased rotational freedom of the substituent groups. It is clear from the above considerations that thermal conversion of a benzene to its *para*-bonded (or other) isomer is only likely to occur in systems where there is a low enthalpy change and a substantial positive entropy change for the process, and that this is most probable where there are many bulky groups attached to the carbon skeleton, as in the case of (1), and also perfluoropentaethylmethylbenzene and perfluoro-1,2,3,5-tetraethyl-4,6-dimethylbenzene.[1]

Nature of the Activated Complex.—The entropies of activation (Table 6) provide particularly useful information about the activated complex for reaction (1). The large positive value of $\Delta S_1^{\ddagger}$ indicates that the activated complex has considerably more freedom of internal motion than the benzene, which can only happen in a configuration which is folded in a similar way to the *para*-bonded isomer. The small negative value of $\Delta S_{-1}^{\ddagger}$ confirms that the complex is not very different in structure from (2). It should be noted that part of the entropy changes are due to the differing symmetries of the species involved. If the pentafluoroethyl group is regarded as a simple substituent, (1) and (2) will have symmetry numbers of 12 and 2 respectively, and the intrinsic overall entropy change for reaction (1) will be decreased by Rln6 (15 J K^{-1} mol^{-1}). If the symmetry number of the activated complex is 2, then the statistical factors, $L^{\ddagger}$ for reactions (1) and (−1) will be 6 and 1 respectively,[8c] and the intrinsic entropy of activation (per reaction path) for the forward reaction will be lower by Rln6. A symmetry number of 12 is the maximum possible for the benzene, and if the ring is non-planar, or the pentafluoroethyl groups exist in restricted configuration, smaller entropy corrections will be appropriate. Such effects therefore make no essential difference to our conclusions about the general structure of the transition state.

The interconversion of (1) and (2) by a concerted disrotatory process is orbital-symmetry forbidden according to the Woodward–Hoffmann rules [14,15] and is therefore

expected to have a high energy of activation. For example, the disrotatory ring opening of *cis*-3,4-dimethylcyclobutene requires an extra energy of at least 60 kJ mol^{-1} above that for the conrotatory process.[16] In the closely related case of a *para*-bonded benzene isomer, however, the conrotatory process, although orbital symmetry allowed, is energetically unfavoured because it would lead to a non-resonant and highly strained *trans*-benzene. Thus, although (2) is much more strained than cyclobutene, the activation energy required for its isomerisation to (1) is larger than that for the ring opening of cyclobutene (138 kJ mol^{-1}),[17] which presumably indicates a different type of mechanism from the concerted conrotatory process accepted for the latter reaction. Since it has been shown that reaction (1) does not involve free radicals, a plausible mechanism for the interconversion process is one involving a biradical intermediate (5) similar to those suggested by Benson

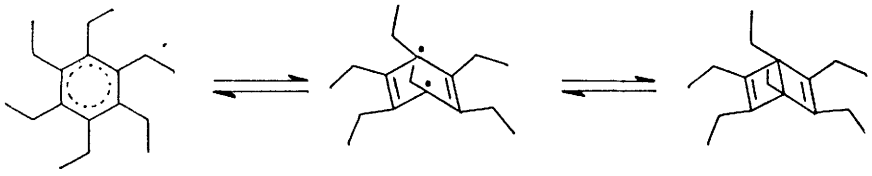

(1) (5) (2)

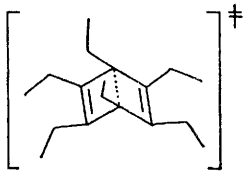

(6)

et al. for the isomerisation of many other polycyclic compounds {in particular bicyclo[2.2.0]hexane and bicyclo[2.2.0]hex-2-ene, which have similar skeletons to (2)}. Semi-empirical calculations of the Arrhenius parameters for such mechanisms have been found to be in good agreement with the experimental data.[18] For this type of mechanism, the overall rate of isomerisation is determined by the rate of conversion of the biradical (5) to the *para*-bonded isomer (2); this proceeds *via* an activated complex which must be (as argued before) similar in structure to (2) rather than (1), and is presumed to have a partial bridge bond as in (6).

Table 9 compares the reported Arrhenius parameters for various *para*-bonded ⟶ benzene isomerisations.

TABLE 9

Arrhenius parameters for the aromatisation of *para*-bonded benzene isomers

Compound	$\log_{10}(A/s^{-1})$	E_a/kJ mol^{-1}	Ref.
(2)	13.0	152	This work
(3a)	15.0	156	9, 10
(3b)	13.2	115	11
(3c)	12.6	161	12
(7), (8)	11.4—14.4	107—128	19, 20

The most reliable data are those for (2) and (3b); these show very similar A factors, and the lower activation energy for (3b) is consistent with greater stabilisation of a biradical intermediate by F compared with C_2F_5. The series designated C_6F_5X refers to the isomeric compounds

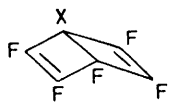

(7)

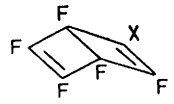

(8)

X = H, Me, CF_3, OMe

(7) and (8); the individual results are not given in detail here since isomer identification was inconclusive and kinetic investigations were restricted (*e.g.* in many cases only one run was performed at each temperature).[19,20] The relative substituent effects in (7) and (8) do however appear to be consistent with the biradical mechanism,[20] and the average A factor is 10^{13} s^{-1}. The high A factor for isomerisation of (3a) may well be attributable to the difficulty of extracting such data from d.s.c. results; an A factor of $10^{13.0}$ s^{-1} would give the same rate at 500 K if the activation energy were 137 kJ mol^{-1}, which is still in line with the other data. Thus a 'normal' A factor of 10^{13} s^{-1} seems well established for these reactions.

[8/1557 *Received*, 25*th August*, 1978]

REFERENCES

[1] Part 9, M. G. Barlow, R. N. Haszeldine, and M. J. Kershaw, *Tetrahedron*, 1975, **31**, 1649.

[2] Preliminary communication, A.-M. Dabbagh, W. T. Flowers, R. N. Haszeldine, and P. J. Robinson, *J.C.S. Chem. Comm.*, 1975, 323.

[3] E. D. Clifton, W. T. Flowers, and R. N. Haszeldine, *Chem. Comm.*, 1969, 1216.

[4] *E.g.*, K. A. W. Parry and P. J. Robinson, *J. Chem. Soc.* (*B*), 1969, 49.

[5] Based on a design used at Leeds University; constructional details available from P. J. R.

[6] W. T. Flowers, R. N. Haszeldine, and J. E. G. Kemp, *Chem. Comm.*, 1969, 203.

[7] P. Sharples, M.Sc. Thesis, Manchester, 1973.
[8] P. J. Robinson and K. A. Holbrook, ' Unimolecular Reactions,' Wiley, London, 1972, (*a*) p. 238; (*b*) p. 152; (*c*) p. 80.
[9] J. F. M. Oth, *Rec. Trav. chim.*, 1968, **87**, 1185.
[10] H. C. Volger and H. Hogeveen, *Rec. Trav. chim.*, 1967, **86**, 830; J. F. M. Oth, *Angew. Chem. Internat. Edn.*, 1968, **7**, 646; W. Adam and J. C. Chang, *Internat. J. Chem. Kinetics*, 1969, **1**, 487.
[11] E. Ratajczak, and A. F. Trotman-Dickenson, *J. Chem. Soc.* (*A*), 1968, 509; I. Haller, *J. Phys. Chem.*, 1968, **72**, 2882.
[12] D. M. Lemal and L. H. Dunlap, *J. Amer. Chem. Soc.*, 1972, **94**, 6562.
[13] M. Randić and Z. Majerski, *J. Chem. Soc.* (*B*), 1968, 1289; M. Randić and Z. Maksić, *Theor. Chim. Acta*, 1965, **3**, 59.
[14] R. B. Woodward and R. Hoffmann, *Angew. Chem. Internat. Edn.*, 1969, **8**, 781.
[15] J. J. Vollmer and K. L. Servis, *J. Chem. Educ.*, 1968, **45**, 214.
[16] J. I. Brauman and W. C. Archie, *J. Amer. Chem. Soc.*, 1972, **94**, 4262.
[17] R. W. Carr and W. D. Walters, *J. Phys. Chem.*, 1965, **69**, 1073.
[18] H. E. O'Neal and S. W. Benson, *Internat. J. Chem. Kinetics*, 1970, **2**, 423.
[19] P. Cadman, E. Ratajczak, and A. F. Trotman-Dickenson, *J. Chem. Soc.* (*A*), 1970, 2109; E. Ratajczak, *Ann. Soc. Chim. Polonica*, 1971, **45**, 257.
[20] E. Ratajczak, *Bull. Acad. Pol. Sci. Ser. Sci. Chim.*, 1973, **21**, 691.